Gynecologic Oncology 153 (2019) 165–174

Contents lists available at ScienceDirect

Gynecologic Oncology

journal homepage: www.elsevier.com/locate/ygyno

# Apatinib exerts anti-tumour effects on ovarian cancer cells

Jing Ding [a], Xiao-yan Cheng [b], Shuang Liu [a], Hong-ying Ji [a], Mu Lin [a], Rong Ma [a,*], Fan-ling Meng [a,*]

[a] Department of Gynecology, Harbin Medical University Cancer Hospital, No. 150 Haping Road, Nangang District, Harbin 150040, Heilongjiang Province, China
[b] Beijing Center for Physical and Chemical Analysis, No. 7 Fengxianzhong Road, Haidian District, Beijing 100094, China

## HIGHLIGHTS

- Apatinib does not appreciably affect the proliferation and vitality of ovarian cancer cells.
- Apatinib inhibits ovarian cancer cells migration.
- Apatinib suppresses the epithelial-mesenchymal transition (EMT).
- Apatinib inhibits the JAK/STAT3, PI3K/Akt and Notch signalling pathways.
- Apatinib inhibits tumour growth in vivo.

## ARTICLE INFO

*Article history:*
Received 12 November 2018
Received in revised form 2 January 2019
Accepted 8 January 2019
Available online 14 January 2019

*Keywords:*
Apatinib
Ovarian cancer
Cell migration
Epithelial-mesenchymal transition
Signalling pathway

## ABSTRACT

*Objective.* Apatinib, a small molecule inhibitor of VEGFR-2 tyrosine kinase, shows strong anti-tumour activity against various tumours. The function of apatinib in ovarian cancer, however, remains unclear. This study was conducted to investigate the effects and potential mechanisms by which apatinib modulates the biological function of ovarian cancer cells in vitro and in vivo.

*Methods.* The effects of apatinib on ovarian cancer cells were determined by assessing cell viability, migration and invasion. The cell cycle distribution and apoptosis of ovarian cancer cells were analysed using flow cytometry. Western blotting was performed to determine the levels of signalling pathway markers. A mouse xenograft model was used to evaluate the efficacy of apatinib in preventing tumour growth.

*Results.* Apatinib did not appreciably affect ovarian cancer cell proliferation and vitality, but did inhibit ovarian cancer cell migration. Apatinib suppressed the epithelial-mesenchymal transition in ovarian cancer cells by inhibiting the JAK/STAT3, PI3K/AKT and Notch signalling pathways. Apatinib effectively inhibited tumour growth in vivo.

*Conclusion.* Based on our findings, apatinib is a highly potent, orally active anti-angiogenic and anti-ovarian cancer agent.



## 1. Introduction

Epithelial ovarian cancer (EOC) is the second most common gynaecologic cancer. It is the most fatal disease and the fifth leading cause of cancer-related death among women [1]. Patients with advanced EOC have a 5-year survival rate of only 40% [2]. The standard treatment for EOC is surgical cytoreduction followed by adjuvant combination chemotherapy. Despite improvements in surgical and chemotherapeutic approaches, the majority of women with relapsed EOC eventually die from the disease, and an unmet and urgent need to improve treatment exists.

Anti-angiogenic therapy is one of the most promising methods for treating cancer. Apatinib, also known as YN968D1, is a new anti-angiogenic therapy agent that has been confirmed to be a safe and effective small-molecule, anti-angiogenic, targeted drug for advanced gastric cancer [3,4]. Independent intellectual property rights for this compound were established in China in 2014. Apatinib is a small-molecule tyrosine kinase inhibitor (TKI) that selectively binds to and potently suppresses VEGFR-2 activity and then blocks VEGFR-2-mediated angiogenesis [5]. As one of the most recently developed oral anti-angiogenic agents, apatinib shows encouraging preclinical and clinical results for the treatment of various solid tumours [5–10].

However, the mechanism underlying the effects of apatinib on ovarian cancer remains unclear. This study was designed to evaluate the effects of apatinib on ovarian cancer cells both in vivo and in vitro and to investigate the characteristics and possible mechanisms of these effects.

* Corresponding authors at: No. 150 Haping Road, Nangang District, Harbin 150040, Heilongjiang Province, China.
*E-mail addresses:* dr_marong2017@126.com (R. Ma), dr_mfl1979@126.com (F. Meng).

https://doi.org/10.1016/j.ygyno.2019.01.010
0090-8258/

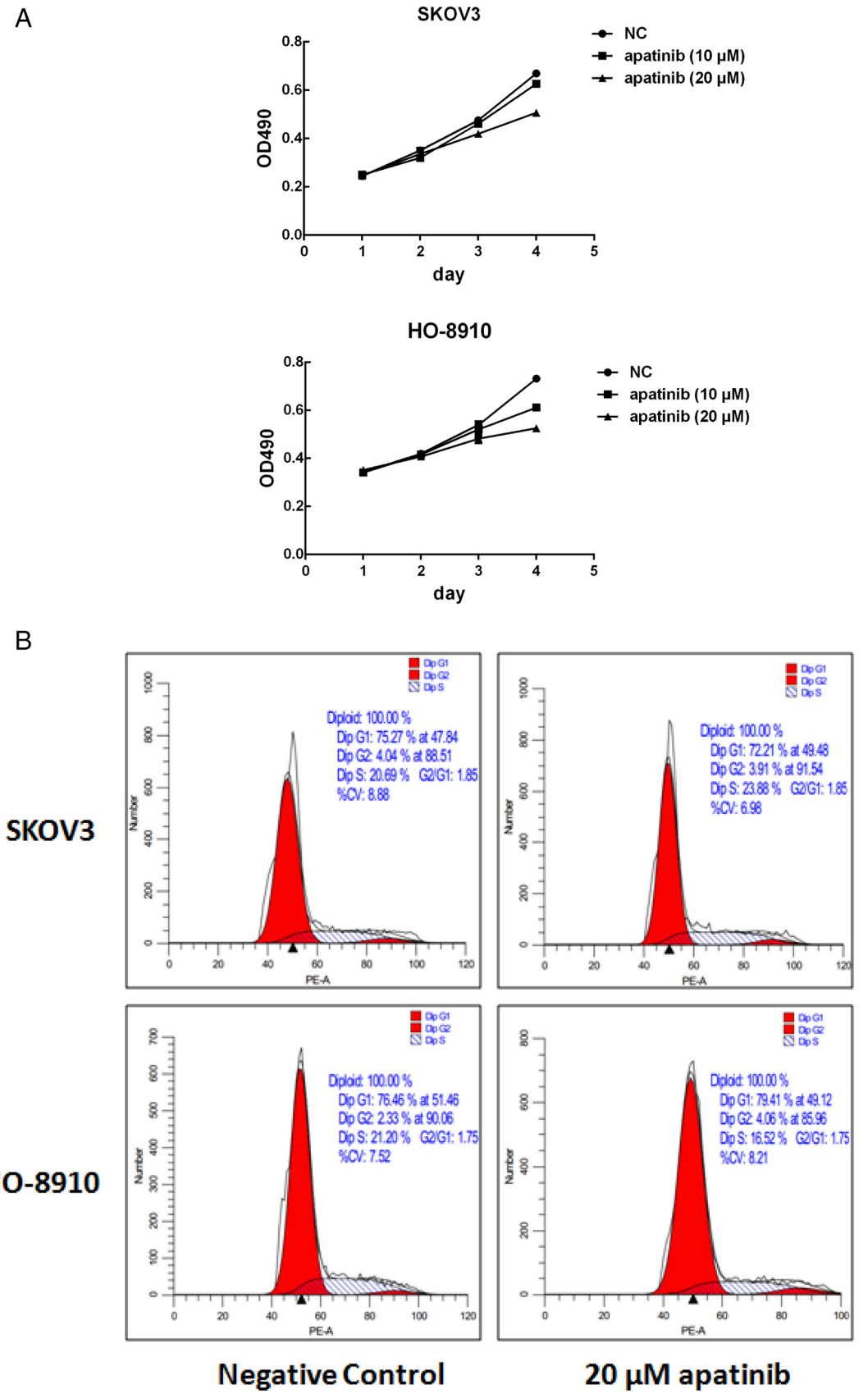


**Fig. 1.** A The effect of apatinib on cell proliferation was determined by the MTT assay. B Flow cytometry assays were conducted to evaluate the effect of apatinib on cell cycle progression. C Flow cytometry assays were conducted to evaluate the effect of apatinib on apoptosis.

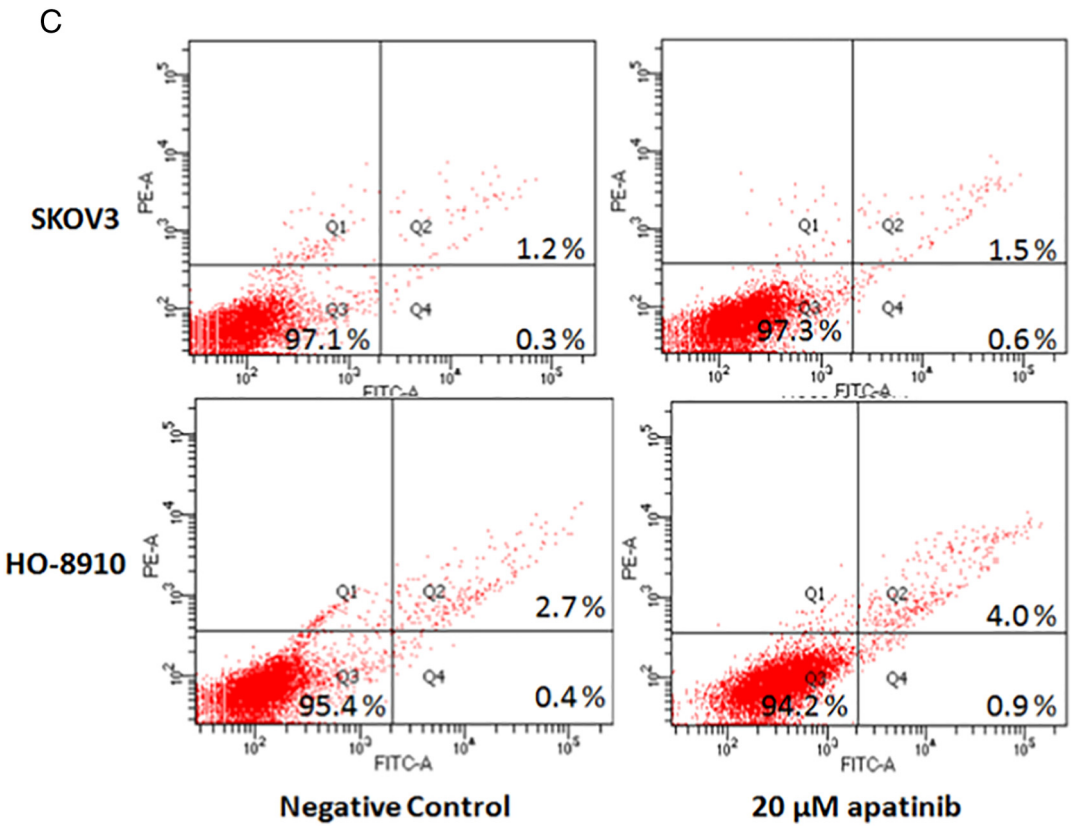


**Fig. 1** (*continued*).

The results are expected to provide experimental data and a theoretical basis for the use of the anti-ovarian cancer agent apatinib in clinical practice.

## 2. Materials and methods

### *2.1. Reagents*

Apatinib was obtained from Hengrui Medicine Co., Ltd. (Jiangsu, China). For the in vitro studies, apatinib was dissolved in 100% dimethyl sulfoxide and diluted to the desired concentration with Dulbecco's Modified Eagle's Medium (DMEM) (Gibco, USA). For the in vivo studies, apatinib was diluted in phosphate-buffered saline.

### *2.2. Cell culture*

The human ovarian cancer cell lines SKOV3 and HO-8910 were obtained from the Cell Bank of Type Culture Collection of the Chinese Academy of Sciences (Shanghai, China). Cells were cultured in DMEM (Gibco, USA) containing 10% foetal bovine serum (FBS; Gibco, USA), 100 U/mL penicillin and 100 μg/mL streptomycin (penicillin-streptomycin-glutamine; Gibco, USA) at 37 °C in a humidified atmosphere of 5% $CO_2$ in a Forma Steri-Cycle $CO_2$ Incubator (Thermo Fisher Scientific, Massachusetts, USA).

### *2.3. Cell proliferation assay*

MTT assays were performed to assess the proliferation of SKOV3 and HO-8910 cells treated with apatinib. SKOV3 and HO-8910 cells were harvested and seeded onto a 96-well plate at a density of $3 \times 10^3$ cells per well. Following a 24-h incubation, cells were treated with 200 μL of culture medium containing apatinib at final concentrations of 10, 20, 50 and 100 μmol/L for 24, 48, 72 and 96 h. Before the assay, the medium was replaced with 100 μL of medium containing 10 μL of MTT (5 mg/mL), and the cells were incubated for an additional 4 h. The absorbance of the solution was measured at 490 nm using a microplate reader (Varioskan Flash, THERMO, USA).

### *2.4. Flow cytometry*

The effects of apatinib on the cell cycle and apoptosis were detected by flow cytometry.

#### *2.4.1. Cell cycle assay*

A flow cytometry analysis was conducted to assay cell cycle arrest in SKOV3 and HO-8910 cells treated with 20 μmol/L apatinib. SKOV3 and HO-8910 cells were seeded onto six-well plates at a density of $3 \times 10^5$ cells per well. Following a 24-h incubation, cells were treated with 20 μM apatinib for 24 h and then subjected to cell cycle assays. Cells were harvested and washed twice with pre-chilled PBS, followed by fixation with 70% ethanol at 4 °C for 2 h. After washes with PBS, cells were stained with 1 μg/mL propidium iodide (PI) (THERMO, USA) in 1 mL of PBS at 4 °C for 30 min. The stained cells were analysed using a flow cytometer (FACS Aria II, BD Biosciences, USA).

#### *2.4.2. Apoptosis assay*

SKOV3 and HO-8910 cells were seeded onto six-well plates at a density of $3 \times 10^5$ cells per well. After a 24-h incubation, cells were treated with 20 μM apatinib for 24 h and then subjected to apoptosis assays. Cells were harvested and washed twice with pre-chilled PBS. Then, a Dead Cell Apoptosis Kit with Annexin V Alexa Fluor® 488 and PI was used to stain the cells for 15 min at room temperature according to the manufacturer's instructions. The stained cells were analysed using a flow cytometer (FACS Aria II, BD Biosciences, USA). FlowJo software was used to analyse and process the results.

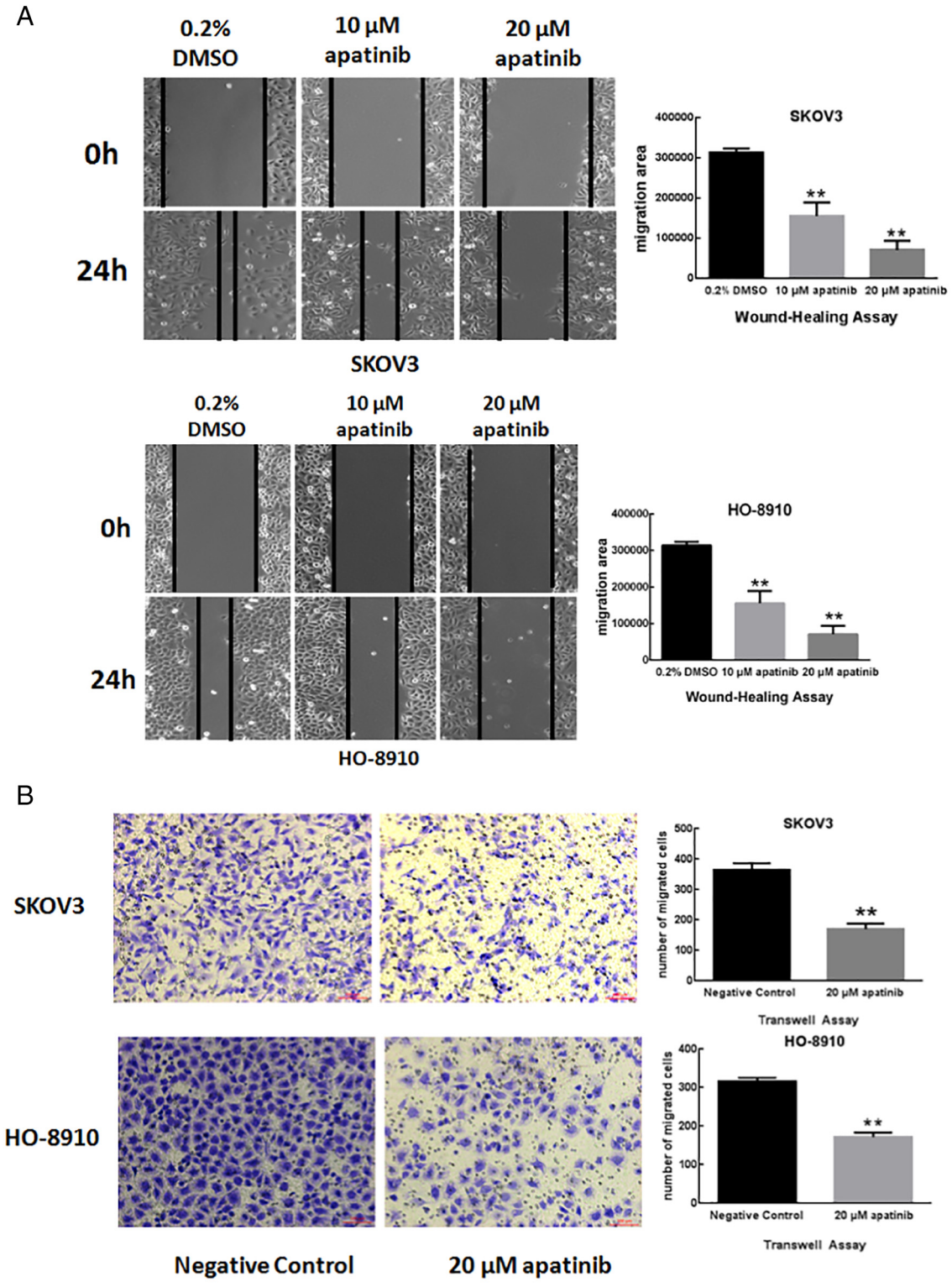


**Fig. 2.** A Apatinib significantly suppressed SKOV3 and HO8910 cell migration, as assessed using wound-healing assays (**P < 0.01). B Apatinib significantly suppressed SKOV3 and HO8910 cell migration, as determined using transwell assays (**P < 0.01). C Apatinib significantly suppressed SKOV3 and HO8910 cell migration, as determined using soft agar assays (**P < 0.01).

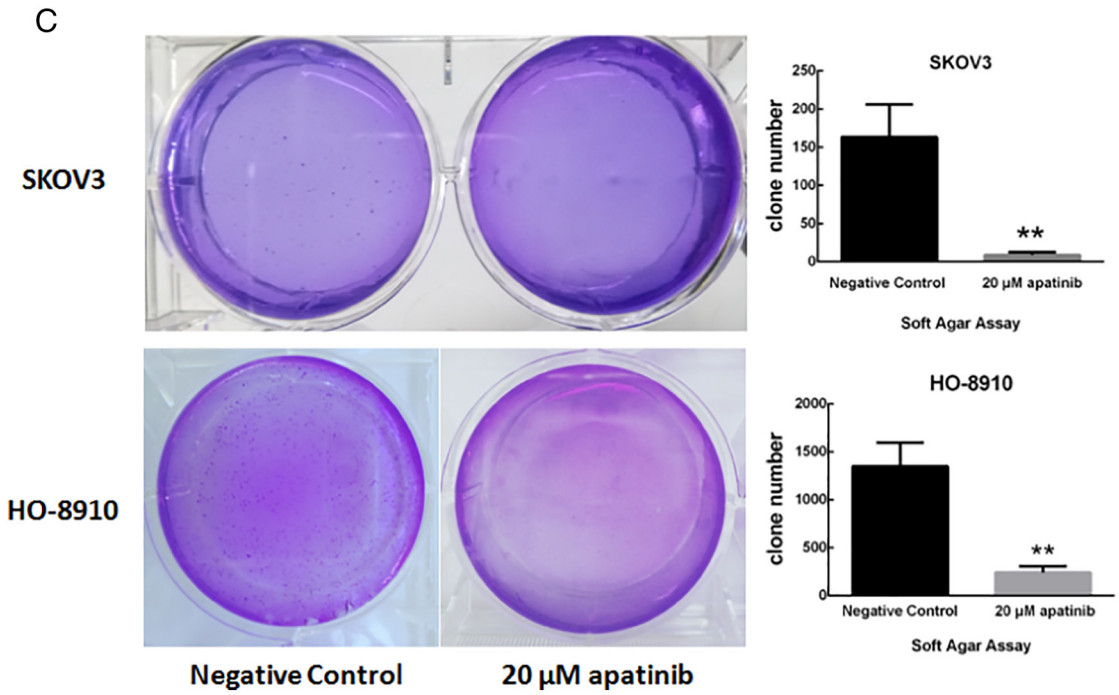


**Fig. 2** (*continued*).

### 2.5. Cell migration

Changes in ovarian cancer migration in vitro after apatinib treatment were detected using scratch wound-healing, transwell and soft agar assays.

#### 2.5.1. Wound-healing assay

SKOV3 and HO-8910 cells were seeded in six-well plates at a density of $5 \times 10^5$ cells per well and allowed to reach 100% confluence prior to the wound-healing assays. The cell layer was wounded with a pipette

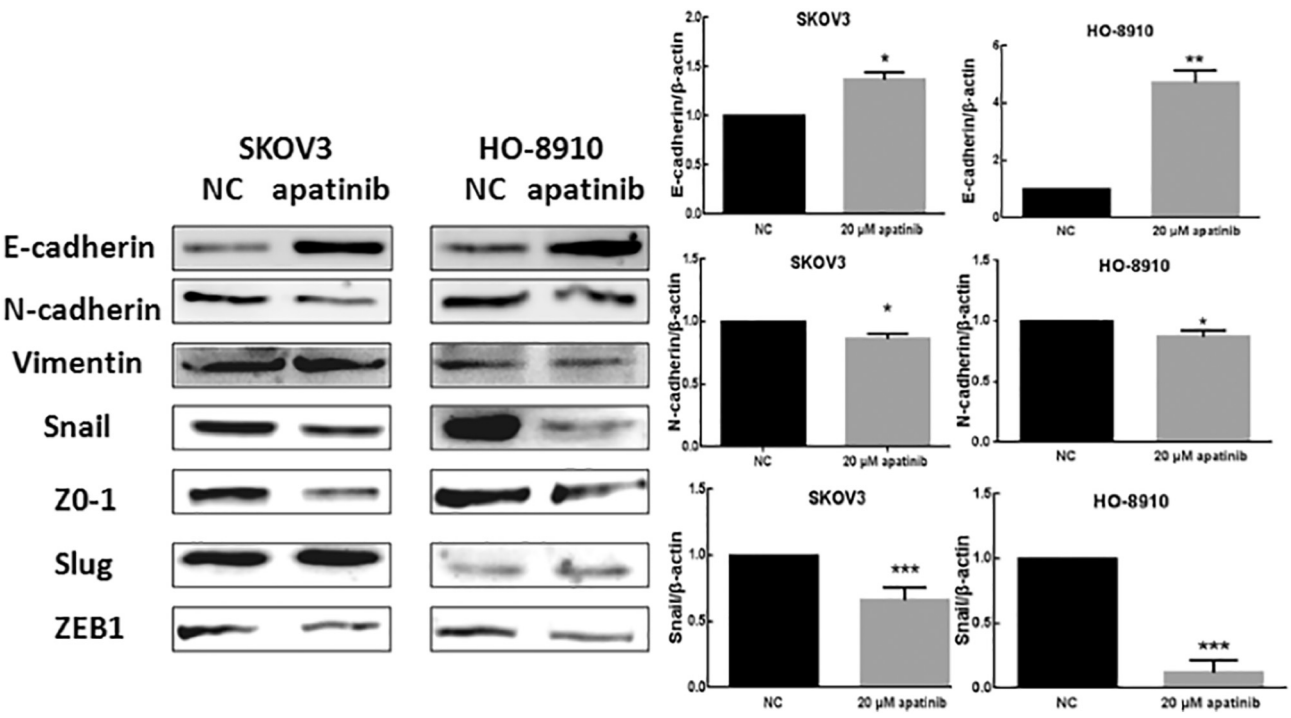


**Fig. 3.** After a 24-h treatment with 20 μM apatinib, protein levels of the EMT markers E-cadherin, N-cadherin, Vimentin, Snail1, Slug, Z0–1 and ZEB1 in Skov3 and HO-8910 cells were determined by western blotting (*P < 0.05; **P < 0.01; ***P < 0.001).

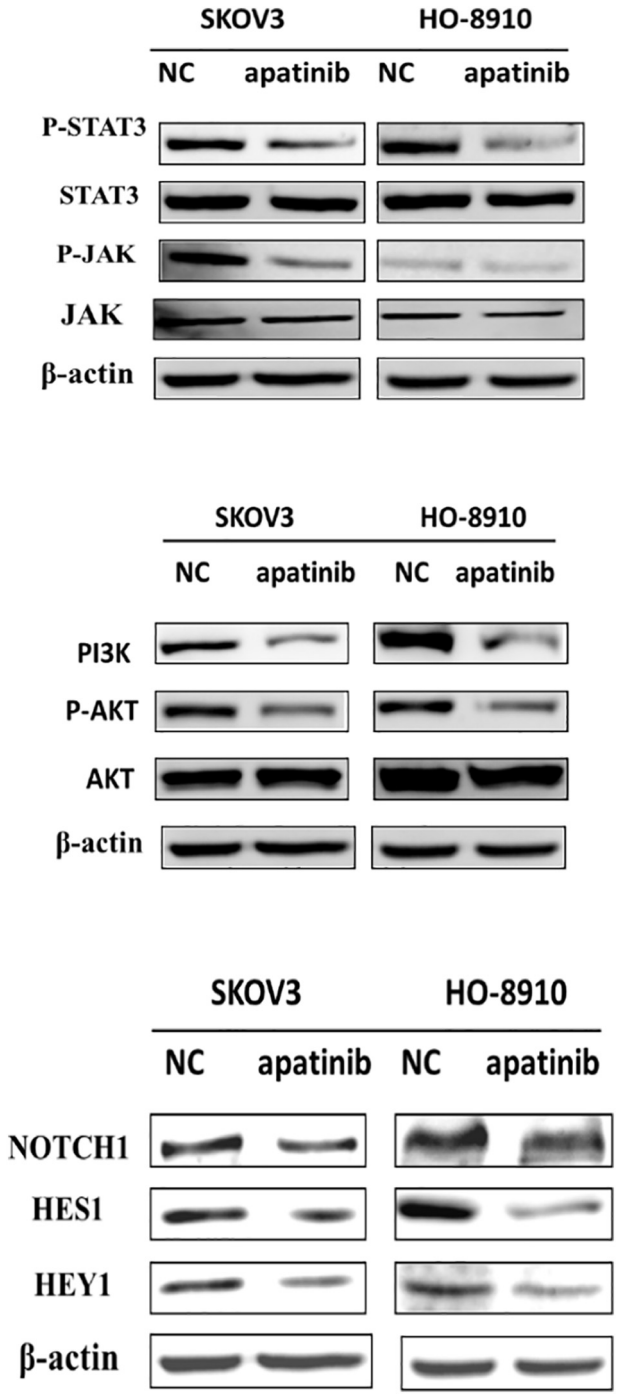


**Fig. 4.** After a 24-h treatment with 20 μM apatinib, the levels of proteins involved in the JAK/STAT3, PI3K/Akt, and Notch signalling pathways, including JAK, p-JAK, Stat3, p-Stat3, PI3K, Akt, p-Akt, Notch1, Hes1 and Hey1, in Skov3 and HO-8910 cells were determined by western blotting.

tip, and the floating cells were removed by two washes with PBS. Cells were then cultured in serum-free DMEM in the presence or absence of apatinib (10 μM and 20 μM) for 24 h, during which the cells were imaged using a live cell imaging system (Zeiss, German). Wound healing was assessed by measuring the distance between the lines of the wounded area under a microscope at 100× magnification.

*2.5.2. Transwell migration assay*

Twenty-four-well transwell chambers (8-μm pore size, 6.5-mm diameter) (Millipore, USA) were used to assay migration and invasion. SKOV3 and HO-8910 cells that had been treated with or without apatinib (20 μM) were harvested and resuspended in serum-free DMEM at a density of $2 \times 10^5$ cells/mL. Next, 100-μL cell suspensions were seeded into the upper chambers of the transwell plates, and 500 μL of DMEM containing 10% FBS were placed in the lower chambers. After co-culture for 24 h, cells on the upper surfaces of the transwell membranes were removed using cotton swabs, and those on the lower surfaces were fixed with ice-cold methanol and stained with a 0.1% crystal violet solution. The number of migrated cells was counted in five random fields.

*2.5.3. Soft agar colony formation assay*

A 6-well plate was coated with a 1:1 ratio of 1.2% agarose and 2× DMEM that was allowed to solidify for 30 min. The top portion was prepared with 0.6% agarose and 2× medium, and SKOV3 and HO-8910 cells that had been treated with or without apatinib (20 μM) were plated at a density of 2000 cells/mL. Images were captured after 14 days of culture.

*2.6. Western blotting*

SKOV3 and HO-8910 cells were seeded onto six-well plates at a density of $3 \times 10^5$ cells per well. Following a 24-h incubation, cells were treated with 20 μM apatinib for 24 h. Then, the cells were harvested, washed twice with pre-chilled PBS, lysed with cell lysis buffer (Beyotime Biotechnology, CHINA) containing 10 mM phenylmethanesulfonyl fluoride (PMSF; Sigma, USA), an EDTA-free protease inhibitor cocktail (Roche, Germany) and PhosSTOP™ (Roche, Germany) for 30 min on ice, and centrifuged at 12,000 rpm for 15 min at 4 °C. The protein concentrations of the supernatants were quantified using a BCA protein assay kit (TIANGEN BIOTECH, CHINA), and equal amounts of protein from each sample were loaded onto gels and separated by sodium dodecyl sulfate-polyacrylamide gel electrophoresis (SDS-PAGE). After separation was complete, the proteins in the gel were transferred onto polyvinylidene fluoride (PVDF) membranes (0.45 μm; Millipore, USA) and blocked with 5% Difco Skim Milk (BD, USA) for 2 h at room temperature. Membranes were subsequently incubated with the indicated primary antibodies at 4 °C overnight. On the next day, membranes were washed with Tris-buffered saline containing 0.1% Tween-20 (TBST, pH 7.4) and incubated with the appropriate secondary antibody at room temperature for 1 h. The immunoblots were detected by enhanced chemiluminescence (ECL, Beyotime Biotechnology, CHINA), and the band densities were analysed using an ImageQuant LAS 4000 system (GE, USA).

*2.7. Mouse xenograft model*

All experiments conformed to the "Guidelines and suggestions for the care and use of laboratory animals" (Ministry of Science and Technology of the People's Republic of China, 2006). The rats were maintained under standard laboratory conditions (20–22 °C, 50–70% relative humidity, 12:12-h light:dark cycle) and had free access to food and water before and after the surgical procedures.

BALB/c-nu/nu mice aged 4–6 weeks and weighing 16–20 g were used to establish the SKOV3 xenograft model. The mice were purchased from Sino-British SIPPR/BK Lab Animal Co., Ltd. (Shanghai, China) and maintained in pathogen-free cages with standard rodent chow and sterile water available ad libitum. Briefly, $5 \times 10^6$ SKOV3 cells were suspended in 200 μL of PBS and inoculated subcutaneously into the right flanks of the nude mice. When the tumours reached a mean diameter of 6 mm, the mice were divided randomly into two groups: control (10% DMSO) and apatinib (50 mg/kg). The mice were intragastrically administered control or apatinib solutions every other day. Throughout the treatment period, the mice were weighed, and their tumours were measured with callipers every 3 days. Tumour volume (V) was calculated using the following formula: $V = \text{largest diameter} \times (\text{smallest diameter})^2/2\ \text{mm}^3$. After 40 days of treatment when the tumours had grown to a proper size, the mice were sacrificed, and the tumours

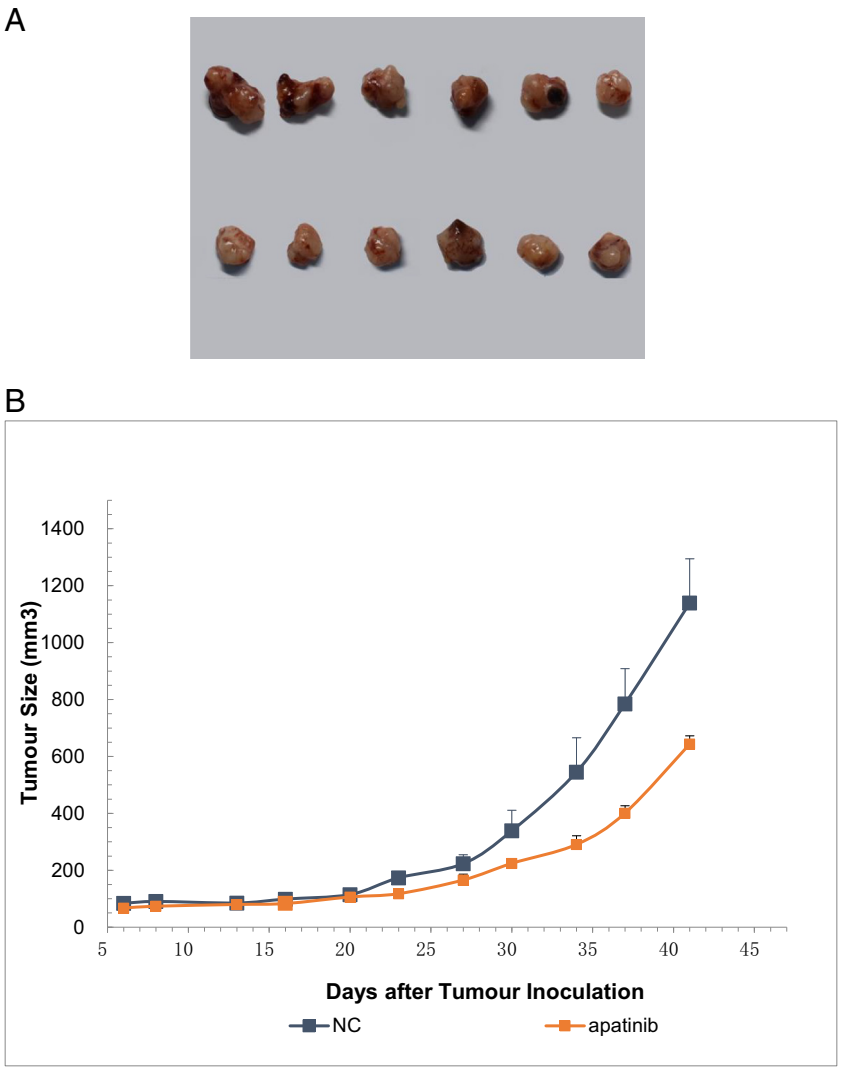


**Fig. 5.** A. Photograph of tumours from the vehicle-treated (upper tissues) and apatinib-treated groups (lower tissues). B. Tumour sizes of SKOV3 ovarian cancer xenografts from mice treated with vehicle (blue curve) and 50 mg/kg apatinib (orange curve).

were excised, weighed and stored at −80 °C or placed in 4% paraformaldehyde for further examination.

### 2.8. Statistical analysis

Each experiment was performed at least three times. Statistically significant differences among groups were evaluated with *t*-tests using SPSS18.0 software. $P < 0.05$ and $P < 0.01$ were considered to represent different levels of statistical significance.

## 3. Results

### 3.1. Apatinib does not appreciably affect the proliferation and vitality of ovarian cancer cells

MTT assays were conducted to determine the effect of apatinib on ovarian cancer cell proliferation. Apatinib did not appreciably affect the proliferation of SKOV3 and HO8910 cells at 10 μM and 20 μM concentrations (Fig. 1A). Flow cytometry was then used to determine the effects of apatinib on cell cycle progression and apoptosis. As shown in Fig. 1B, the percentages of SKOV3 and HO8910 cells in G1/G0 phase were 73.3 ± 2.14% and 73.4 ± 2.69%, in S phase were 22.34 ± 2.17% and 23.64 ± 2.16%, and in G2/M phase were 4.35 ± 0.43% and 2.95 ± 0.53%, respectively. After treatment with 20 μM apatinib, the cell cycle distributions of SKOV3 and HO8910 cells were: G1/G0 phase, 73.04 ± 0.74% and 76.98 ± 2.14%; S phase, 22.79 ± 0.95% and 18.4 ± 1.68%; and G2/M phase, 4.16 ± 0.22% and 4.6 ± 0.46%, respectively. Regarding the effects of apatinib on cell apoptosis, the number of apoptotic cells was not different between SKOV3 and HO8910 cells treated with or without apatinib (Fig. 1C). Apatinib did not appreciably affect the cell cycle progression (Fig. 1B) or apoptosis (Fig. 1C) of SKOV3 and HO8910 cells at concentrations of 20 μM. The 20 μM concentration was selected as the maximum concentration for the subsequent experiments to assay the anti-tumour activity of apatinib.

### 3.2. Apatinib inhibits the migration of ovarian cancer cells

We performed wound-healing, transwell and soft agar assays to determine the anti-tumour activity of apatinib on ovarian cancer cell migration. Apatinib decreased the migratory capacities of SKOV3 and HO8910 ovarian cancer cells at concentrations of 10 μM and 20 μM (Fig. 2A) and 20 μM (Fig. 2B). We then used a soft agar growth assay to investigate the effect of apatinib on the tumourigenesis of SKOV3 and HO8910 ovarian cancer cells. Fewer SKOV3 and HO8910 cell colonies were observed after the 20-μM apatinib treatment than after the control treatment (Fig. 2C). As shown in Fig. 2A–C, the migration and invasion of both SKOV3 and HO8910 cells were significantly reduced following treatment with apatinib ($P < 0.01$).

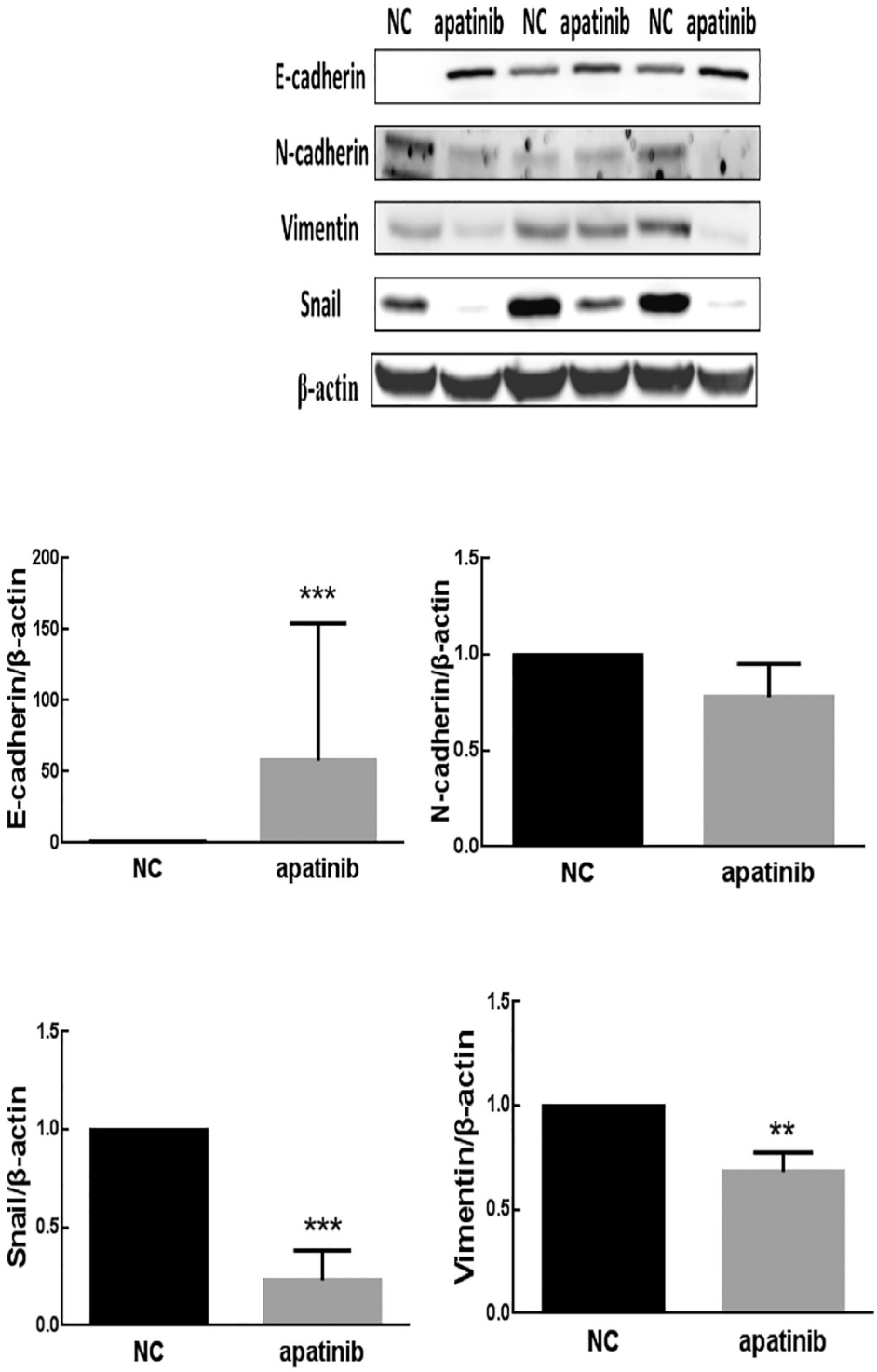


**Fig. 6.** Whole tumour lysates were prepared and protein levels of the EMT markers E-cadherin, N-cadherin, Vimentin, and Snail were analysed by western blotting (**P < 0.01; ***P < 0.001).

### *3.3. Apatinib suppresses the epithelial-mesenchymal transition (EMT) in ovarian cancer cells*

The EMT is closely related to tumour metastasis. Western blotting was performed to measure the levels of EMT-associated markers in SKOV3 and HO8910 cells after treatment with apatinib and investigate whether apatinib suppresses the EMT in ovarian cancer cells. As shown in Fig. 3, the level of the epithelial marker E-cadherin was increased, while the levels of the mesenchymal markers Vimentin and N-cadherin were decreased by the apatinib treatment. Moreover, the levels of the transcription factors Snail and Zo-1 were also decreased by the apatinib treatment. Based on these results, apatinib inhibits the EMT in ovarian cancer cells.

### *3.4. Apatinib inhibits the JAK/STAT3, PI3K/Akt and Notch signalling pathways in human EOC cells*

The JAK/STAT3, PI3K/Akt, and Notch signalling pathways are associated with the EMT. Therefore, western blotting was performed to measure the levels of markers of these three signalling pathways, including

JAK, phosphorylated (p)-JAK, Stat3, p-Stat3, PI3K, Akt, p-Akt, Notch1, Hes1 and Hey1, and to reveal the underlying molecular mechanisms associated with apatinib-induced EMT inhibition in ovarian cancer cells. Apatinib decreased the levels of p-JAK, p-Stat3, p-Akt, PI3K, Notch1, Hey1 and Hes1. JAK, Stat3 and Akt levels were unchanged between the control group and the apatinib-treated group (Fig. 4). Therefore, apatinib inhibits the EMT in human EOC cells via the JAK/STAT3, PI3K/Akt, and Notch signalling pathways.

### 3.5. Apatinib inhibits tumour growth in vivo

After characterizing the effects of apatinib on ovarian cancer cells in vitro, we studied its effect on tumour growth in vivo using a mouse xenograft model. SKOV3 cells were introduced into immunocompromised nude mice to evaluate the efficacy of apatinib in inhibiting tumour growth. As shown in Fig. 5A and B, the oral administration of apatinib significantly inhibited SKOV3 tumour growth compared to the control treatment ($P < 0.05$). Tumour volumes were measured and plotted after each treatment to evaluate the effect of apatinib on mouse xenografts of ovarian cancer cells. After 40 days, the tumour volume of the 50 mg/kg apatinib-treated group ($644 \pm 28.6\ mm^3$) was significantly smaller than the NC group ($1139 \pm 115\ mm^3$) ($P < 0.01$). In this xenograft model of ovarian cancer, apatinib significantly delayed tumour growth in mice. No significant differences in the body weights of the mice were observed between the groups before or after treatment (data not shown).

Tumours were harvested, homogenized, and the levels of downstream protein targets of the drug were analysed using western blotting to further examine target modulation in vivo. As shown in Fig. 6, the level of the epithelial marker E-cadherin was increased, while the levels of the mesenchymal markers Vimentin and N-cadherin were decreased by the apatinib treatment. Moreover, the level of the transcription factor Snail was also decreased by the apatinib treatment. Thus, apatinib inhibits the EMT in mice with ovarian cancer.

## 4. Discussion

As Judah Folkman first proposed in 1971, tumour growth depends on angiogenesis [11]. Inhibitors of angiogenesis have become an important therapeutic strategy in the treatment of various tumours. Tumour angiogenesis plays an important role in the occurrence, development, and metastasis of ovarian cancer. Apatinib is a small-molecule VEGFR TKI that tightly binds and inhibits VEGFR-2 [5]. It is now recognized as a first generation oral anti-angiogenesis drug in China, where it is also a potential new third-line option for treating refractory gastric cancer [12]. Currently, the definitive efficacy of apatinib cannot be estimated due to an insufficient number of patients recruited for clinical trials. However, in many pretreated patients, the survival rates, including overall survival and progression-free survival, have been improved [13]. Apatinib inhibits the migration and proliferation of endothelial cells stimulated by VEGF. Thus, it is considered a promising VEGFR-2 inhibitor that blocks tumour-induced angiogenesis [5,14]. The present study was performed to explore the anti-tumour activity of apatinib in ovarian cancer both in vitro and in vivo. We aimed to provide evidence supporting the use of apatinib as a treatment for ovarian cancer in clinical practice.

Recent studies have reported the direct anticancer activity of apatinib in various cancer cell lines [15,16]. The proliferation of colon cancer cells was inhibited upon treatment with different concentrations of apatinib (20 and 40 μM) [17]. According to the results of the MTT proliferation assay, significantly lower viability of melanoma MUM-2B cells is observed in apatinib-treated groups [18]. In another study, when HCT116 and SW480 cells were treated with 20 μM apatinib, the apoptosis percentages were 3.7% and 5.8%, respectively. As the drug concentration increased to 40 μM, the apoptosis percentages increased to 11.9% and 13.5%. Moreover, the cell cycle was also altered [17]. However, in our study, we did not observe cytotoxic effects of apatinib on ovarian cancer cells. The inhibitory mechanism of apatinib in ovarian cancer cells was further investigated by detecting changes in the cell cycle and cell apoptosis. But, in our study, apatinib did not alter the ovarian cancer cell cycle or cell apoptosis.

In this study, apatinib substantially inhibited the migration and invasion of ovarian cancer cells. (1) Tumour cell motility is an essential factor for tumour invasion and metastasis, and the JAK-STAT3 signalling pathway is commonly over-activated in many physiological cellular pathways involving cell motility [19]. Accordingly, the JAK-STAT3 signalling pathway plays an important role in cell adhesion, migration and other processes. (2) Tumour angiogenesis refers to the growth of capillaries induced by tumour cells and the establishment of blood circulation in tumours. According to previous studies [20,21], STAT3 directly regulates the transcription of VEGF, and the persistent overactivation of the JAK-STAT3 signalling pathway in tumour cells therefore promotes tumour angiogenesis through VEGF, thereby resulting in tumour invasion and metastasis. (3) Degradation of the extracellular matrix (ECM) is a crucial step in tumour invasion and metastasis. The JAK-STAT3 signalling pathway has consistently been shown to be involved in ECM degradation by directly or indirectly regulating the expression of matrix metalloproteinase genes [22]. (4) During the embryonic development of zebrafish, blockade of the K-Ras signalling pathway impairs haematopoiesis and angiogenesis, suggesting that the PI3K/Akt pathway is involved in haematopoiesis and angiogenesis mediated by the K-Ras signalling pathway [23]. Apatinib inhibits the EMT in ovarian cancer cells by inhibiting the JAK/STAT3 and PI3K/Akt signalling pathways to subsequently inhibit ovarian cancer cell motility and invasion, suppress tumour cell volume growth in vivo and indirectly inhibit tumour invasion and metastasis by inhibiting tumour angiogenesis.

## 5. Conclusion

In summary, apatinib significantly inhibits the biological functions of ovarian cancer cells in vitro and in vivo, and our study provided evidence supporting the use of apatinib as a treatment for ovarian cancer in clinical practice.

## Acknowledgments

We are grateful to Mrs. Xiao-yan Cheng for her excellent assistance with these experiments.

All the authors have no conflict of interest.

J Ding: Protocol development, data collection, data analysis and manuscript writing.

X-y Cheng: Data collection, data analysis and manuscript writing.

S Liu: Analysis of tissue responses in the animal model.

H-y Ji: Data collection.

M Lin: Manuscript writing.

R Ma: Protocol development.

F-l Meng: Protocol development.

## References

[1] A. Jemal, R. Siegel, J. Xu, E. Ward, Cancer statistics, CA Cancer J. Clin. 60 (5) (2010) 277–300, https://doi.org/10.3322/caac.20073.

[2] R. Yancik, Ovarian cancer. Age contrasts in incidence, histology, disease stage at diagnosis, and mortality, Cancer 15 (71) (1993) 517–523.

[3] J. Ding, X. Chen, X. Dai, D. Zhong, Simultaneous determination of apatinib and its four major metabolites in human plasma using liquid chromatography-tandem mass spectrometry and its application to a pharmacokinetic study, J. Chromatogr. B 1 (895–896) (2012) 108–115, https://doi.org/10.1016/j.jchromb.2012.03.027.

[4] A.J. Scott, W.A. Messersmith, A. Jimeno, Apatinib: a promising oral antiangiogenic agent in the treatment of multiple solid tumors, Drugs Today 51 (4) (2015) 223–229, https://doi.org/10.1358/dot.2015.51.4.2320599.

[5] S. Tian, H. Quan, C. Xie, et al., YN968D1 is a novel and selective inhibitor of vascular endothelial growth factor receptor-2 tyrosine kinase with potent activity in vitro

and in vivo, Cancer Sci. 102 (7) (2011) 1374–1380, https://doi.org/10.1111/j.1349-7006.2011.01939.x.
[6] J. Li, S. Qin, J. Xu, et al., Apatinib for chemotherapy-refractory advanced metastatic gastric cancer: results from a randomized, placebo-controlled, parallel-arm, phase II trial, J. Clin. Oncol. 31 (26) (2013) 3219–3225, https://doi.org/10.1200/JCO.2013.48.8585.
[7] F. Li, Z. Liao, J. Zhao, et al., Efficacy and safety of Apatinib in stage IV sarcomas: experience of a major sarcoma center in China, Oncotarget 8 (38) (2017) 64471–64480, https://doi.org/10.18632/oncotarget.16293.
[8] X. Hu, J. Cao, W. Hu, et al., Multicenter phase II study of apatinib in non-triple-negative metastatic breast cancer, BMC Cancer 7 (14) (2014) 820–828, https://doi.org/10.1186/1471-2407-14-820.
[9] X. Hu, J. Zhang, B. Xu, et al., Multicenter phase II study of apatinib, a novel VEGFR inhibitor in heavily pretreated patients with metastatic triple-negative breast cancer, Int. J. Cancer 135 (8) (2014) 1961–1969, https://doi.org/10.1002/ijc.28829.
[10] J. Li, S. Qin, J. Xu, et al., Randomized, double-blind, placebocontrolled phase III trial of apatinib in patients with chemotherapy-refractory advanced or metastatic adenocarcinoma of the stomach or gastroesophageal junction, J. Clin. Oncol. 34 (13) (2016) 1448–1454, https://doi.org/10.1200/JCO.2015.63.5995.
[11] J. Folkman, Tumor angiogenesis: therapeutic implications, N. Engl. J. Med. 285 (21) (1971) 1182–1186.
[12] T. Aoyama, T. Yoshikawa, Targeted therapy: Apatinib – new third-line option for refractory gastric or GEJ cancer, Nat. Rev. Clin. Oncol. 13 (5) (2016) 268–2670, https://doi.org/10.1038/nrclinonc.2016.53.
[13] G. Roviello, A. Ravelli, A.I. Fiaschi, M.R. Cappelletti, A. Gobbi, C. Senti, et al., Apatinib for the treatment of gastric cancer, Expert Rev. Gastroenterol. Hepatol. 10 (8) (2016) 887–892, https://doi.org/10.1080/17474124.2016.1209407.
[14] J. Li, X. Zhao, L. Chen, H. Guo, F. Lv, K. Jia, et al., Safety and pharmacokinetics of novel selective vascular endothelial growth factor receptor-2 inhibitor YN968D1 in patients with advanced malignancies, BMC Cancer 5 (10) (2010) 529–536, https://doi.org/10.1186/1471-2407-10-529.
[15] H. Peng, Q. Zhang, J. Li, et al., Apatinib inhibits VEGF signaling and promotes apoptosis in intrahepatic cholangiocarcinoma, Oncotarget 7 (13) (2016) 17220–17229, https://doi.org/10.18632/oncotarget.7948.
[16] C. Lin, S. Wang, W. Xie, R. Zheng, Y. Gan, J. Chang, Apatinib inhibits cellular invasion and migration by fusion kinase KIF5BRET via suppressing RET/Src signaling pathway, Oncotarget 7 (37) (2016) 59236–59244, https://doi.org/10.18632/oncotarget.10985.
[17] W. Lu, H. Ke, D. Qianshan, W. Zhen, X. Guoan, Y. Honggang, Apatinib has anti-tumor effects and induces autophagy incolon cancer cells, Iran J. Basic Med. Sci. 20 (9) (2017) 990–995, https://doi.org/10.22038/IJBMS.2017.9263.
[18] Z.J. Liu, Y.J. Zhou, R.L. Ding, F. Xie, S.Z. Fu, J.B. Wu, L.L. Yang, Q.L. Wen, In vitro and in vivo apatinib inhibits vasculogenic mimicry in melanoma MUM-2B cells, PLoS One 13 (7) (2018) 1–16, https://doi.org/10.1371/journal.pone.0200845 (eCollection 2018).
[19] S. Sano, S. Itami, K. Takeda, M. Tarutani, Y. Yamaguchi, H. Miura, K. Yoshikawa, S. Akira, J. Takeda, Keratinocyte-specific ablation of Stat3 exhibits impaired skin remodeling, but does not affect skin morphogenesis, EMBO J. 18 (17) (1999) 4657–4668.
[20] L.H. Wei, M.L. Kuo, C.A. Chen, C.H. Chou, K.B. Lai, C.N. Lee, C.Y. Hsieh, Interleukin-6 promotes cervical tumor growth by VEGF-dependent angiogenesis via a STAT3 pathway, Oncogene 22 (10) (2003) 1517–1527.
[21] D. Wei, X. Le, L. Zheng, L. Wang, J.A. Frey, A.C. Gao, Z. Peng, S. Huang, H.Q. Xiong, J.L. Abbruzzese, K. Xie, Stat3 activation regulates the expression of vascular endothelial growth factor and human pancreatic cancer angiogenesis and metastasis, Oncogene 22 (3) (2003) 319–329.
[22] F.C. Hsieh, G. Cheng, J. Lin, Evaluation of potential Stat3-regulated genes in human breast cancer, Biochem. Biophys. Res. Commun. 335 (2) (2005) 292–299.
[23] L. Liu, S. Zhu, Z. Gong, B.C. Low, K-ras/PI3K-Akt signaling is essential for zebrafish hematopoiesis and angiogenesis, PLoS One 3 (8) (Aug 6 2008) 1–10, https://doi.org/10.1371/journal.pone.0002850.